Suppression of inelastic collisions of polar $^1\Sigma$ state molecules in an electrostatic field

Alexander V. Avdeenkov,[1] Masatoshi Kajita,[2] and John L. Bohn[3]
[1]*Institute of Physics and Power Engineering, Obninsk, Kaluga Region 249033, Russia*
[2]*National Institute of Information and Communications Technology, 4-2-1 Nukui-Kitamachi, Koganei, Tokyo 184-8795, Japan*
[3]*JILA, NIST, and University of Colorado, Boulder, Colorado 80309, USA*
(Received 11 July 2005; published 6 February 2006)

Collisions of polar $^1\Sigma$ state molecules at ultralow energies are considered, within a model that accounts for long-range dipole-dipole interactions, plus rotation of the molecules. We predict a substantial suppression of dipole-driven inelastic collisions at high values of the applied electric field, namely, field values of several times B_0/μ. Here B_0 is the rotational constant, and μ is the electric dipole moment of molecules. The sudden large drop in the inelastic cross section is attributed to the onset of degeneracy between molecular rotational levels, which dramatically alters the scattering Hamiltonian. This capability could, in principle, be used to stabilize ultracold gases against collisional losses.

DOI: 10.1103/PhysRevA.73.022707 PACS number(s): 34.50.Ez

I. INTRODUCTION

The paramount goal of physics of ultracold temperatures is to control and manipulate the quantum world. Polar molecules bring new challenges and hopes to this field (see the review in Ref. [1]). Since 1998 [2], several experimental groups have been restraining polar molecules in order to get colder and denser samples. The difficulties on this road speak for themselves: a whole variety of experimental techniques were developed for this purpose [1]. But in spite of very intensive experimental research, the production of ultracold molecules still poses a significant challenge. Cold and dense samples would allow one to control two-body [3,4] and many-body systems of polar particles [5–15], although so far none of these goals has been experimentally realized. The main obstacle to these achievements is the loss of trapped molecules via inelastic collisions, or else Majorana transitions [16]. However, given the potentially dominant influence of electric fields on polar molecules, it seems worthwhile to address this influence on collisions. This is the subject of the present paper.

We have previously considered the electrostatic trapping of polar Π-state molecules of both Bosonic (OH) and Fermionic (OD) symmetry from the point of view of stability with respect to collisions [17,18]. As *electrostatic* trapping requires molecules to be in a weak-electric-field seeking state, collisions involving the strong and anisotropic dipole-dipole interaction between molecules may drive the molecules into unfavorable lower-energy strong-field seeking states, leading to unacceptably high trap loss and heating. For Bosonic Π-state OH molecules we have found that the elastic rate can be much larger than the inelastic rate only for quite large field values. As the first excited rotational level of OH lies 84 K above the ground state, inelastic rates are defined mostly by Λ doubling and a hyperfine splitting. In general one cannot yet exclude the possibility of finding molecules whose hyperfine structure suppresses inelastic losses, but such a candidate has not yet been identified.

Polar fermions have a potentially important advantage for electrostatic trapping, namely, low inelastic rates at cold temperatures. The state-changing collisions of dipolar Fermionic molecules were discussed in Refs. [18,19]. Based on the well-known Wigner threshold laws for dipole-dipole interactions it was shown that elastic scattering cross sections are essentially independent of collision energy E at low energies, in electric fields sufficiently strong to polarize the molecules [18]. At the same time, state-changing cross sections scale as $E^{1/2}$ for fermions and as $E^{-1/2}$ for Bosonic molecules. Therefore, at "sufficiently low" temperatures, elastic scattering is always larger for fermions, and evaporative cooling should be possible. Using the first Born approximation (BA), it was concluded [19] that this is the case for the molecules OCS and CH_3Cl, at reasonable experimental temperatures. However, the BA may not be strictly applicable [18] for all fields and energies of interest. Indeed, the Fermi suppression of inelastic collisions may not be of great use for evaporatively cooling the OD radical [18], since "sufficiently low" temperatures in this case turn out to be on the order of 10 nK.

We are therefore motivated in this paper to revisit the question of field-dependent scattering of $^1\Sigma$ Fermionic molecules, from the perspective of close-coupling (CC) calculations. A complete theoretical description of molecule-molecule scattering is complicated by the complexity of the short-range interaction between molecules. This interaction is generally unknown to sufficient accuracy for cold collisions. Therefore in order to avoid the inclusion of unknown parameters of interaction, we seek and explore situations in which the influence of short-range physics is minimal. It appears that for weak-field seeking states the influence of the short-range potential is suppressed, owing to avoided crossings in the long-range interaction [17]. For collisions of identical Fermionic molecules, the influence of short-range physics may be even smaller, since only partial waves with $l \geqslant 1$ are present, and there is a centrifugal repulsion in all scattering channels.

Our point of departure in this paper is the assumption that polar molecules will soon be produced at sub-mK temperatures at sufficient densities to observe collisions. Indeed, samples of RbCs molecules have already been obtained at ~ 100 μK temperatures, in their ground electronic ($^1\Sigma_g$) and vibrational states [20]. These molecules are produced by optical techniques that are believed to be quite general for het-

eronuclear alkali dimers [21]. Thus we consider in this paper the alkali-metal dimers RbCs and RbK. However, as a purely theoretical exercise, we consider several other $^1\Sigma$ molecules. In all cases, we find a strong suppression of inelastic scattering, sometimes by two orders of magnitude, as a function of electric field. We analyze this suppression by looking at adiabatic potential-energy curves of these systems.

II. MODEL

A. Polar $^1\Sigma$-type molecules

The majority of diatomic molecules have $^1\Sigma$ electronic ground states [22]. The energy levels of these species can be described by the rotation J, total spin F (i.e., including nuclear spin), and vibration v quantum numbers. In this paper for simplicity we will neglect hyperfine splitting as the hyperfine interaction for $^1\Sigma$ molecules is smaller than for Π or $^3\Sigma$ molecules and we consider them only in the $v=0$ vibrational ground state. So we will treat polar molecules as rigid rotors with a permanent dipole moment. The Stark splitting will be characterized by (J,M_J), where M_J is the projection of J on the direction of the external electric field. Thus the Hamiltonian for a polar $^1\Sigma$ molecule in a field is

$$H^{1\Sigma} = H_{rot} + H_{field}. \tag{1}$$

The matrix elements for the Hamiltonian (1) in this basis are

$$\langle JM_J|H^{1\Sigma}|J'M_{J'}\rangle = B_0 J(J+1)\delta_{JJ'} - \mu\mathcal{E}(-1)^{M_J}([J] \times [J'])^{1/2}\begin{pmatrix} J & 1 & J' \\ 0 & 0 & 0 \end{pmatrix}\begin{pmatrix} J & 1 & J' \\ -M_J & 0 & M_J \end{pmatrix}. \tag{2}$$

In this expression B_0 is the rotational constant, μ is the molecular dipole moment, $\mathcal{E}$ is the strength of the electric field.

The different values of the molecular rotation J are strongly mixed in laboratory strength fields. Accordingly, in practice we transform the molecular state to a field-dressed basis for performing scattering calculations:

$$|(\tilde{J})M_J;\mathcal{E}\rangle \equiv \sum_J \alpha(J)|JM_J\rangle, \tag{3}$$

where $\alpha(J)$ stands for eigenfunctions of the Hamiltonian (1) determined numerically at each value of the field. The J quantum number is not a good quantum number in a field, but we will continue to refer to molecular states with $\tilde{J}$ as a reminder of the zero-field value of J.

Figure 1 shows the Stark energies computed using all the ingredients described above. In zero field the energy levels are determined by the rotational constant B_0. We demonstrate the Stark splitting for linear OCS molecule which is quite typical for this type of molecule. For the other molecules we consider, the figure would look exactly the same, but with rescaled axes. We estimated that the hyperfine splitting is of order of μK, which means that this effect may be important for ultracold energies. But here we will ignore the hyperfine effects as the region of energies we are considering is quite above μK. The Stark shift is quadratic for fields below the

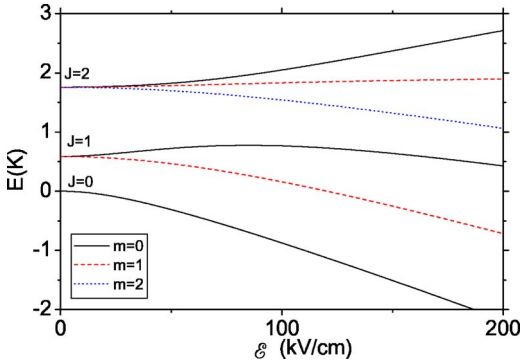

FIG. 1. (Color online) Stark effect for linear OCS molecules in their $^1\Sigma$ ground state.

"critical field" defined by $\mathcal{E}_0 \equiv B_0 J(J+1)/2\mu$. It is a rather approximate estimate because of the mixing between the neighboring rotation levels. For a molecule in its lowest weak-field seeking state $|10\rangle$ the critical electric field is typically on the order of 10^3–10^4 V/cm for the species we consider here. For fields larger than this, the states with $J=0$, 1, 2 are deeply mixed. As a consequence, a state like $|10\rangle$, which is weak-field seeking in low fields, can become high-field seeking at somewhat higher fields. In the following, as we are interested in $J=1$ states, the critical field is given by $\mathcal{E}_0 = B_0/\mu$.

B. Dipole-dipole interaction

The intermolecular dipole-dipole interaction has the form

$$V_{\mu\mu}(\mathbf{R},\omega_1,\omega_2) = \frac{\boldsymbol{\mu}_1\cdot\boldsymbol{\mu}_2 - 3(\hat{\mathbf{R}}\cdot\boldsymbol{\mu}_1)(\hat{\mathbf{R}}\cdot\boldsymbol{\mu}_2)}{R^3} = -\frac{\sqrt{6}}{R^3}\sum_q (-1)^q C^2_{-q}(\omega)[\mu_1\otimes\mu_2]^2_q, \tag{4}$$

where $\omega_{1,2}=(\theta_{1,2},\phi_{1,2})$ are the polar angles of molecules 1 and 2 with respect to the lab-fixed quantization axis, and $\mathbf{R}=(R,\omega)$ is the vector between the center of mass of the molecules in the laboratory fixed coordinate frame. Here $C^2_{-q}(\omega)$ is a reduced spherical harmonic [23].

We express the Hamiltonian in a basis of projection of total angular momentum,

$$\mathcal{M} = M_{J_1} + M_{J_2} + M_l; \tag{5}$$

M_l is the projection of the partial wave quantum number l on the laboratory axis. In this basis the wave function for two molecules is described as

$$\Psi^{\mathcal{M}} = \frac{1}{R}\sum_{1,2,l,M_l}\{|1\rangle\otimes|2\rangle\otimes|lM_l\rangle\}^{\mathcal{M}}\psi^{\mathcal{M},1,2}(R), \tag{6}$$

where $\{\cdots\}^{\mathcal{M}}$ is the angular momentum part of this wave function and $|i\rangle$ is the wave function for each molecule. As we consider the target and the projectile as identical molecules, we must take into account the symmetry of the wave function (6) under exchange.

Taking into account the Wigner-Eckart theorem, we can present the reduced angular matrix element as

$$\langle 12lM_l\|A_\Lambda\|1'2'l'M_{l'}\rangle = (-1)^{M'_{J_1}+M'_{J_2}+M_l-1}([l][l'][J_1][J'_1][J_2][J'_2])^{1/2}\begin{pmatrix} 1 & 1 & 2 \\ M_{J_1}-M_{J'_1} & M_{J_2}-M_{J'_2} & M_l-M_{l'}\end{pmatrix}\begin{pmatrix} J'_1 & 1 & J_1 \\ 0 & 0 & 0\end{pmatrix}$$
$$\times\begin{pmatrix} J'_2 & 1 & J_2 \\ 0 & 0 & 0\end{pmatrix}\begin{pmatrix} 1 & J_1 & J'_1 \\ M_{J_1}-M_{J'_1} & -M_{J_1} & M_{J'_1}\end{pmatrix}\begin{pmatrix} 1 & J_2 & J'_2 \\ M_{J_2}-M_{J'_2} & -M_{J_2} & M_{J'_2}\end{pmatrix}\begin{pmatrix} l' & L & l \\ M_{l'} & M_l-M_{l'} & -M_l\end{pmatrix}$$
$$\times\begin{pmatrix} l' & 2 & l \\ 0 & 0 & 0\end{pmatrix}. \tag{7}$$

In practice, before each scattering calculation the Hamiltonian matrix has to be transformed from this basis into the field-dressed basis defined by Eq. (3). We solve the coupled-channel equations using a logarithmic derivative propagator method [24] to calculate total state-to-state cross sections. Since the projection of total angular momentum on the field axis, $\mathcal{M}$, is a conserved quantity, calculations can be performed for each value of $\mathcal{M}$ separately. We find, generally, that the dominant contribution to cross sections arises from the minimum allowed value of $\mathcal{M}$ and that the general behavior of cross sections for other $\mathcal{M}$ is quite similar, and so restrict calculations accordingly.

The scattering calculations quickly become computationally expensive as more rotational states and partial waves are included. Because we need to calculate cross sections at many electric field values, we choose a "compromise" basis set that includes rotational levels up to $J_{max}=3$ and partial waves up to $L_{max}=3$. This basis set then consists of 182 scattering channels. The basis with $J_{max}=4$ and $L_{max}=5$ already contains 681 channels. The influence of the basis on the effect we found is discussed in Fig. 7. This level of approximation tends to get the general magnitude of elastic scattering cross sections fairly accurately, and to *overestimate* inelastic scattering cross sections. We therefore expect to draw conservative conclusions on the high ratio of elastic to inelastic scattering.

III. RESULTS AND DISCUSSION

We have chosen a variety of different linear molecules for this study, to span a range of rotational constants and dipole moments, and also to connect with the results of Ref. [19]. Properties of the molecules are summarized in Table I [25,26]. Of particular interest is the alkali dimer RbCs and RbK, which are leading candidates in the experimental quest to observe cold collisions [20,29]. For these molecules, we are interested in the lowest energy weak-field seeking state of the ground vibrational state, $|JM_J\rangle=|10\rangle$ (see Fig. 1). In contrast to the Π molecules we have previously studied [27,28], here it is necessary to include several rotational levels of the molecule.

TABLE I. Molecular parameters for the species considered. The rotational constants B_0 and dipole moments μ for the triatomics come from Ref. [25], while those for RbCs and RbK come from Refs. [26,31]. Here $\mathcal{E}_0=B_0/\mu$ is the "critical" field, while $\mathcal{E}_{\text{supp}}$ is the calculated field value at which the inelastic processes become suppressed.

Molecule	B_0 (cm^{-1})	μ (D)	$3\mathcal{E}_0$ (kV/cm)	$\mathcal{E}_{\text{supp}}$
RbCs	0.017	1.26	2.35	2.55
RbK	0.0382	0.76	8.98	9.8
ClCN	0.199	2.833	12.57	13.65
OCS	0.203	0.715	50.71	55.3
HCN	1.478	2.985	88.51	96.4

The general behavior of the thermally averaged cross sections versus temperature is shown in Fig. 2. This example is for ClCN molecules in an electric field of $\mathcal{E}=20$ kV/cm, well above the critical field for this molecule, meaning that the molecule is strongly polarized. The heavy solid and dashed lines represent (respectively) the elastic and state-changing cross sections for fermionic isotopomers of this molecule. It can be seen that the standard threshold behavior of colliding dipoles occurs at energies below several tens of μK. Namely, the elastic cross section becomes a constant, and the inelastic cross section goes to zero as $T^{1/2}$ [18,19]. By contrast, the light solid and dashed curves show the same quantities, but for a Bosonic isotopomer. Here the threshold laws work against the experimentalist, with the inelastic rate diverging as $T^{-1/2}$ [17,19]. At higher temperatures, above the threshold regime, the elastic and inelastic cross sections are comparable for both bosons and fermions, consistent with what was found for OH and OD radicals in Ref. [18].

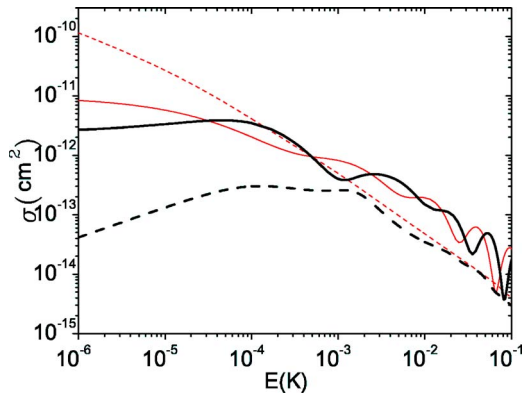

FIG. 2. (Color online) Elastic (solid lines) and inelastic (dashed lines) cross sections for ClCN molecule at an electrostatic field $\mathcal{E}=20\,000$ V/cm. Thick and thin curves are for Fermi and Bose particles, respectively.

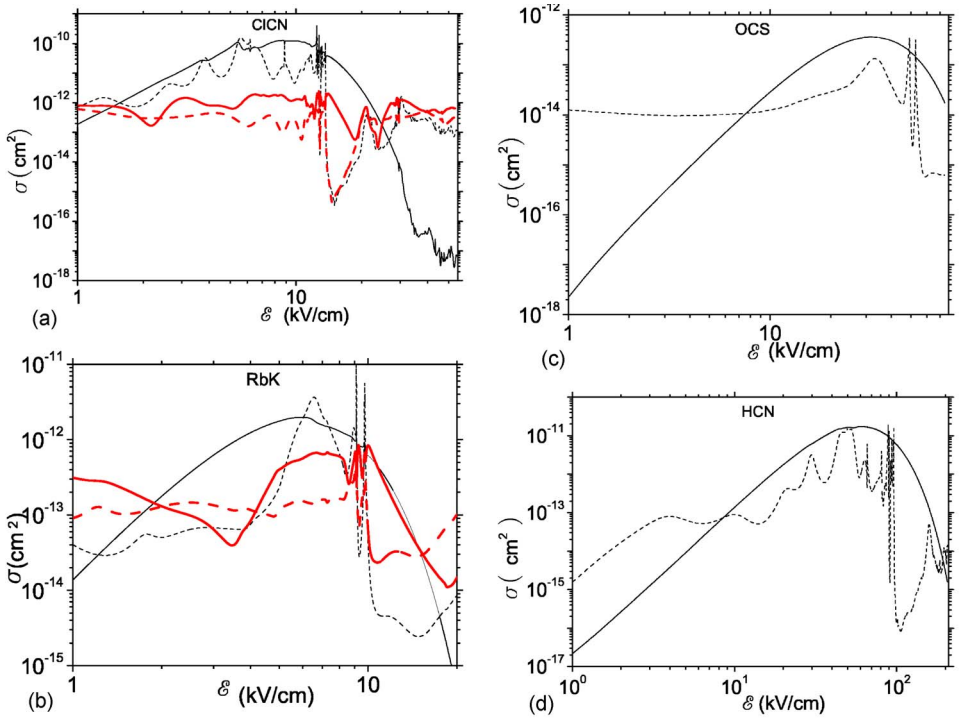

FIG. 3. (Color online) Elastic (solid lines) and inelastic (dashed lines) cross sections versus an electrostatic field at collision energy 1 μK for (a) ClCN, (b) RbK, (c) OCS, and (d) HCN molecules. Thick lines are for cases at collision energy 1 mK. For these calculations, $L_{max}=3$, $J_{max}=3$.

Remarkably, this situation can change quite dramatically if the electric field takes certain values. We illustrate this in Fig. 3, by plotting elastic and inelastic cross sections at $T=1$ μK and 1 mK, versus electric field. In each case, the inelastic cross sections (dashed lines) fall by two to four orders of magnitude at a specific value of the electric field. Here we show only results for Fermionic species. For Bosonic species the corresponding drop is smaller because of the threshold behavior at this energy. The field values at which this suppression occurs, denoted $\mathcal{E}_{\text{supp}}$, are tabulated in Table I. In all cases the suppression occurs at around three times the critical field $\mathcal{E}_0$. To explore this phenomenon further, we focus on a particular example in the following, namely, a Fermionic isotopomer of ClCN.

The unexpected suppression of inelastic collision rates has its origin in the interplay between the strong dipole-dipole interaction and the rotational energy levels of the molecules. The first clue to the mechanism of suppression comes from considering the scattering thresholds, i.e., the total energy of both molecules when they are far apart (Fig. 4). Here each threshold is labeled according to the quantum numbers $|J_1M_1,J_2M_2\rangle$ of the colliding molecules, and zero energy represents the lowest energy threshold corresponding to $|00, 00\rangle$. The solid line denotes the $|10, 10\rangle$ incident channel of interest to this paper. It can be seen here that this threshold crosses three other thresholds, for the channels $|00, 22\rangle$, $|00, 21\rangle$, and $|00, 20\rangle$, at fields $\mathcal{E}=11.6, 12.8, 13.65$ kV/cm, respectively, very near $\mathcal{E}_{\text{supp}}$. As we will see below, $\mathcal{E}_{\text{supp}}$ can be defined more quantitatively as the field at which thresholds for the channels $|10, 10\rangle$ and $|00, 20\rangle$ are degenerate.

This is a strange situation, in which the state-changing collision cross sections *diminish* sharply just as new states become energetically available. The second piece to this puzzle is found by examining the approximate adiabatic potential-energy curves for two situations, as shown in Fig. 5. To simplify these curves, we have included only the partial wave $L=1$ in their construction, although $L=3$ is also used in the multichannel scattering calculations. In Fig. 5(a) are shown the curves for $\mathcal{E}=12.3$ kV/cm, just below the threshold crossing. Here the incident channel $|10, 10\rangle$ is below the nearby thresholds, and correlates adiabatically to the solid curve. This curve draws molecules into the small-R region where they interact strongly and can readily change their internal state.

By contrast, Fig. 5(b) shows the adiabatic curves at a field $\mathcal{E}=13.7$ kV/cm, just above the threshold crossing. Now the

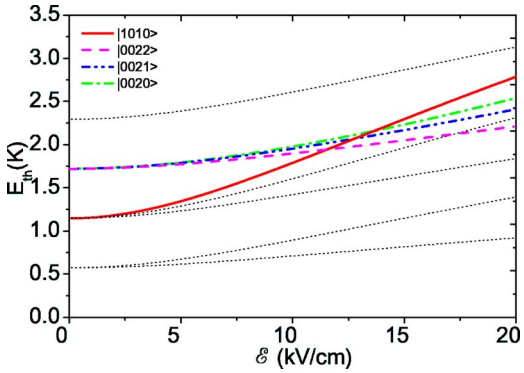

FIG. 4. (Color online) Threshold energies for ClCN molecules referred to the threshold of the $|00, 00\rangle$ channel. Dotted curves are for some other channels.

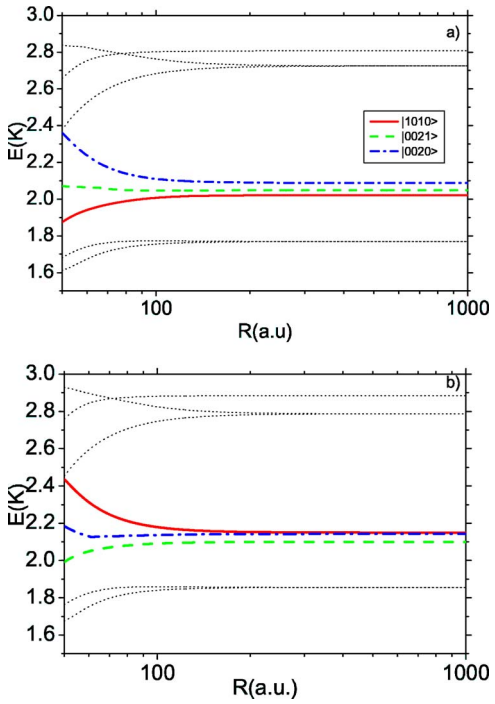

FIG. 5. (Color online) Adiabatic curves for ClCN molecule at (a) 12.3 kV/cm and (b) 13.7 kV/cm. In both cases the dark curve correlates adiabatically to the $|10\rangle|10\rangle$ incident channel at large R. Dotted curves are for some other channels.

incident channel correlates adiabatically to a repulsive curve, so that the molecules do not approach one another nearly as closely as in the previous case. This shielding, in turn, reduces the likelihood of inelastic collisions. The dominance of the repulsive curve is a peculiarity of the strong, anisotropic dipole-dipole interaction, and is similar to the physics that generates "field-linked" molecular dimer states, which also keep the molecules far from each other [28]. While this simple picture of the suppression is probably a good first approximation, there is clearly more going on. This can be seen in the tabulated values of $\mathcal{E}_{\text{supp}}$, which are not always equal to $3\mathcal{E}_0$, even though this is the field value where the thresholds cross for any $^1\Sigma$ molecule.

It should be noted that molecules with comparable values of $\mathcal{E}_0$ will have quite different suppression of inelastic scattering. This can be seen in Figs. 3(a) and 3(b), which compare ClCN and RbK molecules. These molecules have very similar values of $\mathcal{E}_0$ but RbK has a notably smaller dipole moment and rotational constant. This suggests that at 1 mK a "weaker" polar rigid rotor such as RbK experiences a less favorable elastic to inelastic ratio than ClCN molecules.

We also remark that we have noted a similar, but somewhat less dramatic, suppression of inelastic cross sections in Bosonic analog of the molecules considered (Fig. 6). Presumably fermions have an advantage since they have nonzero partial wave angular momentum in all channels, which aids in the shielding effect discussed above. Although there are no naturally occurring Fermionic RbCS molecules we performed calculations for them with the same parameters as for Bosonic molecules for a methodical purpose.

The strong suppression in the low-energy limit naturally has consequences at higher collision energies. Figure 7

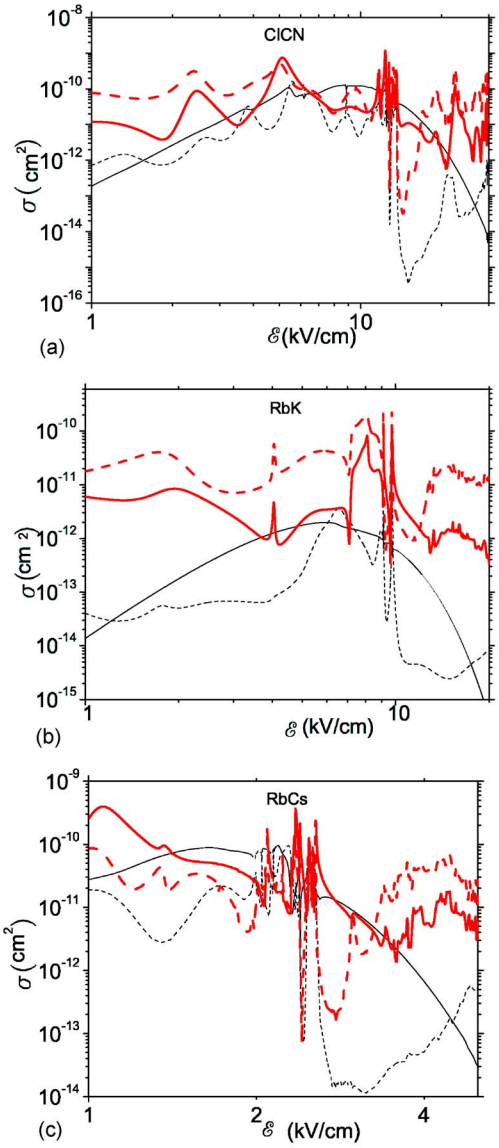

FIG. 6. (Color online) Elastic (solid lines) and inelastic (dashed lines) cross sections versus electrostatic field at collision energy 1 μK for (a) ClCN, (b) RbK molecules, and (c) RbCs. The thick curves are for Bosons particles and thin curves are for Fermion particles, respectively. $M_{tot}=0$.

shows the elastic (solid) and inelastic (dashed) cross sections versus temperature, at a field $\mathcal{E}=14$ kV/cm, where the inelastic rates have just become suppressed. Strikingly, the ratio of elastic to inelastic cross sections is close to two orders of magnitude even at temperatures as high as several mK, which is attainable in photoassociation experiments. For this reason, it is conceivable that if cold, dense samples are produced, they may be amenable to evaporative cooling that will reduce them to ultracold temperatures. An already ultracold gas may also be stabilized against collisional losses by this effect.

Figure 7 also illustrates the effect of increasing the number of channels in the scattering calculations. For both elastic (solid lines) and inelastic (dashed lines) cross sections, four curves are shown, corresponding to various maximal num-

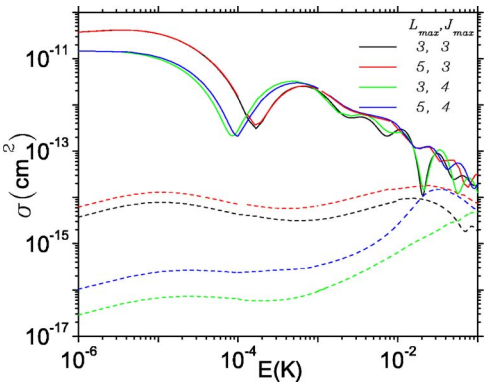

FIG. 7. (Color online) Elastic (solid lines) and inelastic (dashed lines) cross sections versus the collisional energy for ClCN molecule. J_{max} and L_{max} are maximal taken into account values of rotation an partial quantum numbers. The electrostatic field is 14 kV/cm.

bers of rotational states (J_{max}) and partial waves (L_{max}). In all cases, changing the size of the basis set has little influence on the overall elastic scattering cross section, although the features understandably shift in field. By contrast, the inelastic cross sections are quite sensitive to J_{max}, dropping more than an order of magnitude as J_{max} increases from 3 to 4. In addition, the number of partial waves plays a role in the actual cross sections. In any event, the conclusions still hold, and the ratio of elastic to inelastic cross sections should be quite high.

IV. CONCLUSION

In this paper we considered the collisional dynamics of polar $^1\Sigma$ molecules in a dc-electric field using ClCN, HCN, OCS, RbCs, and RbK as examples. As a rule the strong and anisotropic dipole-dipole interaction provides quite large inelastic rates. We have found, however, that polar $^1\Sigma$ state molecules possess a substantial suppression of inelastic collisions at high values of the applied electric field. The sudden drop in inelastic cross section coincides with the degeneracy of certain molecular rotational levels. Adiabatic pictures reveal that the interaction changes from mostly attractive to mostly repulsive upon crossing the field where this coincidence occurs. The strong suppression of inelastic scattering from the $|JM_J\rangle = |10\rangle$ state of a $^1\Sigma$ molecule seems generally to occur at a field nearly equal to $3B_0/\mu$. This phenomenon will be of great interest to study experimentally, as a dramatic consequence of electric fields on scattering at ultralow energies.

As a final remark, we note that in many experiments alkali dimer molecules are formed in high-lying vibrationally excited states, as a result of photoassociation or magnetoassociation. In these quite different states, the field scale can be significantly larger. To make an estimate, consider the RbK molecule, which is being pursued by the UConn group and at JILA [30,31]. In a hypothetical weakly bound state whose outer turning point is 40 a.u., this molecule's rotational constant is approximately $B_0 = 1.4$ cm^{-1}. The dipole moment of this molecule has been estimated to be approximately $1.4 \times 10^{-5} e a_0$ at this intermolecular separation [31], yielding a critical field of $\mathcal{E}_0 \approx 2$ MV/cm. Thus it would seem unlikely that the effects described here are observable for such weakly bound molecules. For even more weakly bound molecules, the critical field quickly becomes larger, owing to the exponential falloff of the dipole moment.

ACKNOWLEDGMENTS

This work was supported by the NSF and by a grant from the W. M. Keck Foundation.

[1] J. Doyle *et al.*, Eur. Phys. J. D **31**, 149 (2004).
[2] J. D. Weinstein, R. deCarvalho, T. Guillet, B. Friedrich, and J. M. Doyle, Nature (London) **395**, 148 (1998).
[3] N. Balakrishnan and A. Dalgarno, Chem. Phys. Lett. **341**, 652 (2001).
[4] E. Bodo, F. A. Gianturco, and A. Dalgarno, J. Phys. B **35**, 2391 (2002).
[5] L. You and M. Marinescu, Phys. Rev. A **60**, 2324 (1999).
[6] K. Goral, B-G. Englert, and K. Rzazewski, Phys. Rev. A **63**, 033606 (2001).
[7] M. A. Baranov *et al.*, Phys. Rev. A **66**, 013606 (2002).
[8] M. A. Baranov *et al.*, Phys. Scr., T **T102**, 74, (2002).
[9] M. A. Baranov, L. Dobrek, and M. Lewenstein, Phys. Rev. Lett. **92**, 250403 (2004).
[10] S. Yi and L. You, Phys. Rev. A **61**, 041604(R) (2000).
[11] L. Santos *et al.*, Phys. Rev. Lett. **85**, 1791 (2000).
[12] S. Yi and L. You, Phys. Rev. A **63**, 053607 (2001).
[13] K. Goral and L. Santos, Phys. Rev. A **66**, 023613 (2002).
[14] S. Giovanazzi, A. Gorlitz, and T. Pfau, Phys. Rev. Lett. **89**, 130401 (2002).
[15] D. H. J. O'Dell, S. Giovanazzi, and C. Eberlein, Phys. Rev. Lett. **92**, 250401 (2004).
[16] M. Kajita, T. Suzuki, H. Odashima, Y. Moriwaki, and M. Tachikawa, Jpn. J. Appl. Phys., Part 2 **40**, L1260 (2001).
[17] A. V. Avdeenkov and J. L. Bohn, Phys. Rev. A **66**, 052718 (2002).
[18] A. V. Avdeenkov and J. L. Bohn, Phys. Rev. A **71**, 022706 (2005).
[19] M. Kajita, Phys. Rev. A **69**, 012709 (2004).
[20] J. M. Sage, S. Sainis, T. Bergeman, and D. DeMille, Phys. Rev. Lett. **94**, 203001 (2005).
[21] W. C. Stwalley, Eur. Phys. J. D **31**, 221 (2004).
[22] G. Herzberg, *Molecular Spectra and Molecular Structure: I. Spectra of Diatomic Molecules* (Van Nostrand, Princeton, 1950).
[23] D. M. Brink and G. R. Satchler, *Angular Momentum*, 3rd ed. (Oxford University Press, New York, 1993).
[24] B. R. Johnson, J. Comput. Phys. **13**, 445 (1973).

[25] http://physics.nist.gov/PhysRefData/MolSpec/
[26] G. Igel-Mann, U. Wedig, P. Fuentealba, and H. Stoll, J. Chem. Phys. **84**, 5007 (1986).
[27] A. V. Avdeenkov and J. L. Bohn, Phys. Rev. Lett. **90**, 043006 (2003).
[28] A. V. Avdeenkov, D. C. E. Bortolotti, and J. L. Bohn, Phys. Rev. A **69**, 012710 (2004).
[29] D. Wang *et al.*, Phys. Rev. Lett. **93**, 243005 (2004).
[30] D. Jin (private communication).
[31] S. Kotochigova, P. S. Julienne, and E. Tiesinga, Phys. Rev. A **68**, 022501 (2003).